





Characterization, Measurement and Specification of Device Imperfections in Optical Coherent Transceivers

Zhenning Tao , Senior Member, IEEE, Yangyang Fan , Xiaofei Su, Ke Zhang, Chengwu Yang, Tong Ye , Jingnan Li , Hisao Nakashima, and Takeshi Hoshida, Senior Member, IEEE

(Invited Paper)

Abstract—Transceiver imperfections become the primary source of impairment as baud rate and modulation order grow in advanced optical coherent communications. Thus, transceiver imperfections, both linear and nonlinear, need to be appropriately characterized, measured, and specified. Treatments for linear imperfections are relatively mature. This study reviews the transceiver’s linear imperfection modeling, characterization, and measurement technologies. In practical applications, in-field measurement using the transceiver and a few low speed additional devices is preferred. In the case of nonlinear imperfections, the situation is complex. One important task is to estimate the nonlinear system performance from the nonlinear characteristics of the devices. In this study, we attempt to establish a connection between them by examining different technologies. Although the orthogonal component has a good correlation with nonlinear system performance, its measurement is prohibitively complex. In the nonlinear noise to power ratio measurement, a certain frequency component of the input signal is notched, and the re-growth component at the notch frequency is measured at the nonlinear device output. The ratio between the re-growth component power and the output signal power is the noise to power ratio. While this method is easy to carry out, it does not correctly estimate nonlinear impairment in general. The reason for this is that the signal incurs different nonlinear responses in two conditions, i.e., with or without a notch. This method accurately estimates the nonlinear impairment in some special but useful cases, such as Gaussian input signals and nonlinear systems whose dominant nonlinear term is the even order term.

Index Terms—Device imperfection, imperfection measurement, nonlinear specification, optical coherent transceiver, optical communication.

Manuscript received November 12, 2021; revised January 29, 2022; accepted February 17, 2022. Date of publication March 1, 2022; date of current version May 25, 2022. (Corresponding author: Zhenning Tao.)

Zhenning Tao, Yangyang Fan, Xiaofei Su, Ke Zhang, Chengwu Yang, Tong Ye, and Jingnan Li are with the Fujitsu Research and Development Center, Beijing 100022, China (e-mail: taozn@fujitsu.com; fanyangyang@fujitsu.com; suxiaofei@fujitsu.com; zhangke@fujitsu.com; yangchengwu@fujitsu.com; yetong@fujitsu.com; lijingnan@fujitsu.com).

Hisao Nakashima and Takeshi Hoshida are with the Fujitsu Limited, Kawasaki 212-8510, Japan (e-mail: nakashima.hisao@fujitsu.com; hoshida@fujitsu.com).

Color versions of one or more figures in this article are available at <https://doi.org/10.1109/JLT.2022.3155454>.

Digital Object Identifier 10.1109/JLT.2022.3155454

I. INTRODUCTION

WITH the increase of network traffic, optical communication uses a higher baud rate and higher modulation order. For example, a 304 GBaud polybinary modulation for intensity modulation and direct detection (IM/DD) system was demonstrated in [1]. For coherent transmission, a 220 GBaud quadrature phase shift keying (QPSK) signal was generated by two-channel 256 GSa/s arbitrary waveform generator [2]. A 160 GBaud eight quadrature amplitude modulations (QAM) was generated by an ultra-broadband optical frontend module integrated with a bandwidth multiplexing function [3]. In terms of modulation order, 15 GBaud 2048QAM transmission over 100 km was demonstrated in [4], and 130 GBaud dual-polarization probabilistic constellation shaped 256QAM transmission was reported in [5]. In such high speed and high order modulation systems, the device imperfections turn out to be significant [6]. In addition, the major network traffic occurs in the metro and data-center networks. In such application, transmission impairments such as fiber nonlinearity are insignificant, whereas device imperfection turns out to be the primary source of impairment [7]. Thus, it’s necessary to characterize, measure, and specify the device imperfections in optical transceivers.

Device imperfections could be categorized into linear and nonlinear imperfections. The linear imperfections could be sufficiently characterized by the frequency transfer function. The problem is how to effectively measure the transfer function with limited resources in different scenarios [8]. In terms of nonlinear imperfections, the situation is complex. There have been various nonlinear specifications, such as total harmonic distortion (THD), inter-modulation ratio, gain compression, and nonlinear noise to power ratio (NPR) [9]. A fundamental challenge is that nonlinear impairment does not only depend on the nonlinear device itself, but also depends on input signal characteristics, such as signal power, spectrum, and probability distribution function (PDF). The test signal used in the nonlinearity specification is generally different from the signal in actual communication operations. Thus, it is not easy to accurately estimate nonlinear system performance from nonlinear specifications.

In [8], we briefly reviewed the linear and nonlinear device imperfection modeling, characterization, and measurement for

optical coherent transceivers. In this study, we extend the linear imperfection part with an additional detailed explanation and examples. We extend the nonlinear part by discussing how to connect nonlinear device specifications and nonlinear system performance. The orthogonal component has a good correlation with nonlinear system performance, but the measurement is difficult. NPR is easy to measure, but it does not always correctly predict nonlinear system performance. In some special but useful cases, such as Gaussian input signals and nonlinear systems whose dominant nonlinear term is the even order term, NPR has a good correlation with nonlinear system performance.

II. DEVICE LINEAR IMPERFECTIONS

Linear imperfection is the basic impairment in communication systems. In this section, we will review the sources, the model, and the measurement of linear imperfections in optical coherent transceivers. The major challenge is how to effectively measure the imperfections with limited resources in real applications.

A. Overview of Linear Imperfections and Measurement

In coherent transceivers, there are many electrical or electro-optical devices, and each device has its own linear transfer function. Those transfer functions sufficiently describe the device's linear characteristics, and the overall transfer function is the product of all those individual functions. One important fact is that the coherent transceiver has two separate tributaries, i.e., an in-phase (I) tributary and a quadrature (Q) tributary. The characteristics of the I and Q branches may be different, so that the single-input-single-output (1×1) complex transfer function cannot sufficiently describe the transceiver linear characteristics. The matrix with two inputs and two outputs (2×2) should be used [10]. Additionally, the model based on the matrix with 2×2 real signal transfer function was named the "widely linear model," whereas that based on the 1×1 complex signal transfer function was the "strictly linear model" [11].

The block diagram of one polarization tributary of a coherent transmitter and the sources of linear imperfections is shown in Fig. 1. Each I or Q branch has its own frequency amplitude and phase response. The difference between the I and Q branches is known as an IQ imbalance. The frequency independent imbalance consists of a constant amplitude imbalance, a constant phase imbalance, and a skew. The frequency dependent imbalances contains the amplitude and phase imbalances [12]. An IQ imbalance causes frequency image distortion and is the most significant linear distortion in transceivers [13].

Device imperfection measurement is a key task in real applications. It is the basis of imperfection compensation, device specification, and transceiver assessment. There are three different application scenarios where the available measurement resources are different.

The first one is the measurement in a factory or laboratory. In this case, there are expensive measurement instruments such as vector network analyzers and high-resolution spectrum analyzers. With the help of such instruments, the device imperfections could be measured accurately.

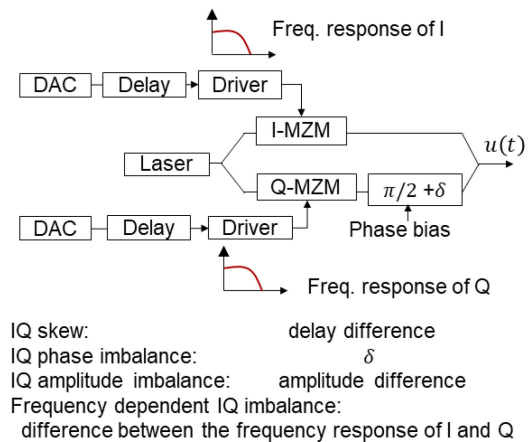


Fig. 1. Linear imperfections in coherent transceivers, taking one polarization tributary of the transmitter as an example.

The second case is in-field measurement before transmission service is provided. In this case, the available hardware for measurement is the transceiver itself. Anyway, there are still some amounts of memory attached to the digital to analog converter (DAC) in the transmitter and the analog to digital converter (ADC) in the receiver because digital signal processing (DSP) chip testing and debugging need those memories. Such memory plus the DAC/ADC constitutes a light version of an arbitrary waveform generator (AWG) and a digital storage oscilloscope (DSO). In addition, there is the freedom to design the measurement process and the test signal. Based on those two functionalities, many researchers have proposed various algorithms.

The third one is in-field measurement after transmission service is provided. In this case, only very limited resources, such as training sequences, could be freely designed. Fortunately, the receiver DSP operates in this case, and the device imperfections can be measured by analyzing the coefficients of the adaptive linear equalizer.

B. Device Imperfection Measurement in the Laboratory

With the help of various instruments, device imperfection measurement is not very difficult in a laboratory or factory. In principle, the vector network analyzer with an electrical and optical interface could measure the linear transfer function precisely. Besides this, there are several proposals using less expensive instruments. The methods to measure the transmitter frequency amplitude response and IQ skew with the assistance of a high-resolution optical spectrum analyzer are shown in Fig. 2. The digital flat comb signal is sent to one tributary and zeros are sent to other tributaries as shown in Fig. 2(a). The measured output optical spectrum is the frequency dependent amplitude response of that tributary [14]. The comparison of I and Q tributaries obtains the IQ amplitude imbalance. The digital single side band (SSB) comb signal is used, and the IQ skew is measured by analyzing the slope of the image spectrum. The result is shown in Fig. 2(b) [15]. Alternatively, if we notch the digital $I+jQ$ signal at a positive frequency but do not notch at

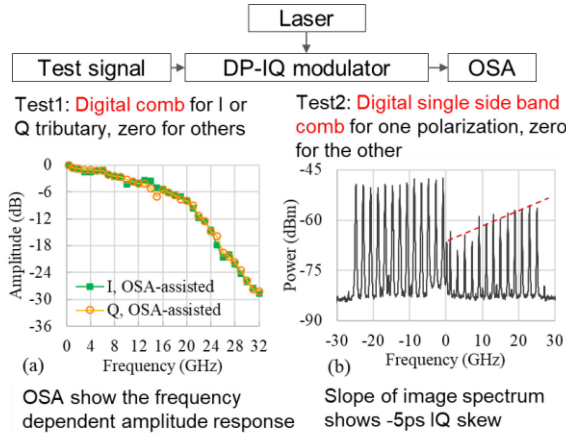


Fig. 2. Transmitter frequency amplitude response and IQ skew measurement in the laboratory. DP: dual-polarization, OSA: optical spectrum analyzer.

the corresponding negative frequency, the notched SSB signal is generated. The IQ skew could also be measured by analyzing the optical output spectrum [16]. On the receiver side, if we connect the white noise source to the receiver, the digital spectrum of each ADC's samples shows the frequency dependent amplitude response of the corresponding tributary [17]. For receiver IQ skew, the proposal in [18] feeds a continuous waveform (CW) laser to the receiver and adjusts the frequency offset with a local oscillator. Then, the phase difference between I and Q branch is estimated, and skew is the slope of the phase difference to the frequency offset.

C. In-Field Measurement Before Service

In-field measurement is much more challenging than that in a laboratory or factory, but it is highly needed because the device imperfections in the field may be different from those in a factory due to environmental change. Lots of methods have been proposed using the transceiver's light version AWG, DSO, and additional resources. Among them, the methods using fewer additional resources are preferred.

One good example is transmitter amplitude response measurement without any additional high speed devices [19]. The block diagram of the proposed method is shown in Fig. 3. The response of different tributaries is measured one by one, so Fig. 3 only shows the process of one tributary. The overall amplitude response is the concatenated response of the DAC, driver, and E/O response of the Mach-Zehnder modulator (MZM). If we have a digital single tone with amplitude A and frequency f_i , the electrical signal before the ideal MZM has the amplitude $AG(f_i)$, where $G(f_i)$ is the amplitude response to be measured. In the transmitter, there is always a low speed photo detector (PD) to monitor the average output power. There is one important fact: the average output power $P_{av,i}$ has a fixed relationship with the input electrical signal amplitude $AG(f_i)$. The relationship is affected by many parameters, such as PD responsivity, electrical swing, V_π of phase modulation, and such parameters change from piece to piece. As a result, the relationship was unknown before the measurement. In the first step, we calibrate the

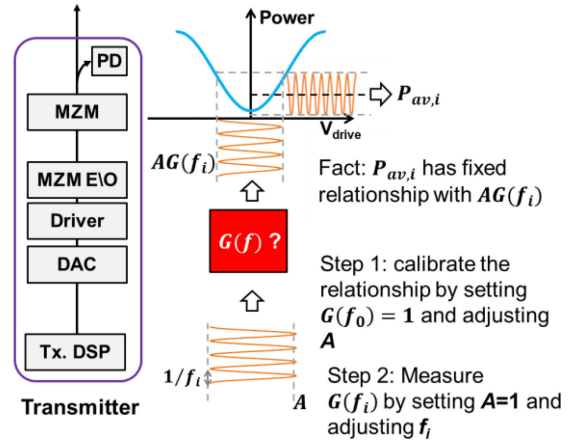


Fig. 3. Transmitter frequency dependent amplitude response measurement by the built-in low speed monitor photo detector.

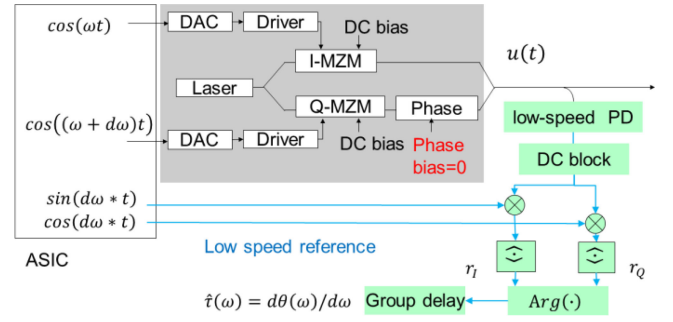


Fig. 4. Transmitter frequency dependent IQ phase imbalance measurement by the built-in low speed monitor photo detector and low speed DSP.

relationship by setting a low frequency f_0 having $G(f_0) = 1$ and adjusting amplitude A . In the second step, we set the amplitude $A = 1$, adjust the frequency f_i , and measure the average output power $P_{av,i}$. Using the calibrated relationship in step 1, we could calculate the amplitude response $G(f_i)$ from $P_{av,i}$. The IQ amplitude imbalance may be easily obtained with the amplitude responses of I and Q.

Another example is transmitter frequency dependent IQ phase imbalance calibration without any additional high speed device [20]. The block diagram of the proposed method is shown in Fig. 4. In this approach, the digital signals of the I and Q branches are two synchronized tones, i.e., $\cos(\omega t)$ and $\cos(\omega t + d\omega t)$. After the DAC, driver, and E/O response of MZM, the I and Q branch signals before the ideal MZM are $A_I(\omega)\cos(\omega t + \theta_I(\omega))$ and $A_Q(\omega)\cos(\omega t + d\omega t + \theta_Q(\omega + d\omega))$, where $\theta_{I/Q}(\omega)$ is the phase response, and $A_{I/Q}(\omega)$ is the amplitude response. In real operation, the IQ phase bias is $\pi/2$, but in the calibration process it is 0. Then, the output optical signal is $A_I(\omega)\cos(\omega t + \theta_I(\omega)) + A_Q(\omega)\cos(\omega t + d\omega t + \theta_Q(\omega + d\omega))$. The square operation of PD generates several beating items, and there is a differential frequency beating item $A_I(\omega)A_Q(\omega)\cos(-d\omega t + \theta_I(\omega) - \theta_Q(\omega + d\omega))$. This item has a low frequency $d\omega$ and could be detected by the low speed PD. Its phase is the IQ phase imbalance $\theta_I(\omega) - \theta_Q(\omega + d\omega) \approx \theta_I(\omega) - \theta_Q(\omega)$. Finally, the

low speed synchronized detection obtains the IQ phase imbalance. One important trick in this approach is that the low speed reference $\cos(d\omega t)$ and high speed signal $\cos(\omega t)$ should be synchronized.

Employing a similar idea, the transmitter frequency dependent phase response was measured without any high speed device [21]. In this approach, two synchronized digital tones $\cos(\omega t)$ and $\cos(\omega t + d\omega t)$ are sent into one tributary, whereas all the other tributary signals are zero. The output optical signal is $A(\omega)\cos(\omega t + \theta(\omega)) + A(\omega + d\omega)\cos(\omega t + d\omega t + \theta(\omega + d\omega))$ which is very similar to that of [20]. Then, the left process is the same. In order to relax the strict synchronization request of high speed tone and low speed reference signal, the segment-splice method was proposed in [21].

Another example of calibrating transmitter IQ skew was shown in [22]. In this approach, the same binary phase shift keying signal is fed to both the I and Q branches in the transmitter. During calibration, the IQ phase bias is set to π , instead of $\pi/2$. If there is no IQ skew, the I and Q branch signals cancel each other out, and the average output power is at its minimum. This method has a large calibration range, but the resolution is relatively low.

The four examples above only use transmitters, low speed devices, and low speed DSP. If high speed devices and DSP are used, there are more proposals. Using high speed PD and ADC, the transmitter frequency dependent IQ amplitude, phase imbalance, and skew were simultaneously estimated via widely linear phase retrieval [23]. Using a delay interferometer, high speed balanced PD, and high speed ADC, the transmitter frequency dependent IQ amplitude and phase imbalance were measured by employing an elaborate IQ stimulus that forms self-coherent detection [24].

If the transmitter and receiver are jointly used, more approaches have been proposed. The transmitter and receiver IQ skew can be simultaneously obtained after receiver side DSP by feeding the IQ interleaved multi-tone stimulus into the transmitter IQ tributaries [25]. The transmitter IQ skew is estimated from the coefficient of transmitter adaptive digital pre-distortion by indirect learning architecture and the feedback signal after receiver carrier recovery [26]. The transmitter generates a real valued optical comb signal by sending the digital comb signal into one branch of the transmitter. If there is a frequency offset, each tone splits into two tones after beating with the local laser at the receiver. Then, receiver IQ response and imbalance could be estimated based on receiver DSP [27]. By employing the unitary polarization change matrix, both transmitter and receiver polarization skews are simultaneously measured by analyzing the receiver adaptive equalizer coefficient [28]. Several machine learning methods were proposed in [29]–[31].

D. In-field Measurement After Service

We still need the device imperfection measurement after the transmission service is provided. The primary motivation is to monitor the transceiver status. As long as the adaptive equalizer operates successfully, it is straightforward to

monitor receiver device imperfections by analyzing the equalizer coefficients [10], [32], [33]. It's worthwhile to notice that the adaptive equalizer before carrier phase recovery simultaneously compensates for the receiver imperfections, transmission link distortion, and the common part of transmitter response. Thus, only the receiver's IQ imbalance could be monitored by the 2×2 widely linear equalizer.

The receiver side DSP could also monitor the transmitter device imperfections. If there is a frequency offset, the transmitter's I and Q signals are mixed from the receiver's point of view. Thus, the receiver's constant modulus algorithm passes the transmitter IQ imbalance. After carrier phase recovery, the I and Q signals are separated again, and the 2×2 widely linear equalizer compensates and monitors the transmitter IQ imbalance [12], [34]–[36]. Besides the adaptive equalizer, the clock recovery algorithm detects the time error and monitors the skew [37], [38].

Since the channel condition changes much slower than the baud rate, the required monitor speed is much lower than the baud rate. Consequently, the monitor function could be realized in an off-line software manner but not in a real time hardware manner. As a result, the algorithm complexity is not a big issue.

E. Summary of Device Linear Imperfections

Device linear imperfections are the basic impairment in the transceiver. Since it is linear, the transfer function sufficiently describes the imperfection characteristic. The 2×2 real signal transfer function matrix, instead of the 1×1 complex signal transfer function, should be used, because the imperfections occur at the I and Q branches separately. The IQ imbalance causes the crosstalk between the I and Q branches, and it is the major linear impairment in the transceiver. Device imperfection measurement is the basis for compensation, specification, and assessment. Considering the available resources for measurement, there are three typical scenarios, i.e., laboratory application, in-field measurement before service, and in-field measurement after service. Table I summarizes various measurement methods under three scenarios.

III. DEVICE NONLINEAR IMPERFECTIONS

Device nonlinear imperfections are another kind of important impairment in transceivers. Nonlinear compensation is widely studied to overcome them [1], [2], [4], [5]. Besides that, understanding the nonlinear imperfections themselves is also an important task. Compared with linear imperfections, nonlinear imperfections are much more complicated. In this section, we will review the sources of nonlinear imperfections in coherent transceivers, the model of nonlinear imperfections, and the specification of nonlinear imperfections. The major topic is how to connect device nonlinear characteristics and nonlinear system performance when there is no nonlinear compensation.

TABLE I
SUMMARY OF TRANSCEIVER DEVICE LINEAR IMPERFECTION MEASUREMENT

Measurement objects	Required resources	Principle	Reference
Laboratory measurement			
Tx amp. resp.	HR OSA	Using a digital comb input signal at one tributary, measure the optical output spectrum.	14
Tx IQ phs. imb. & skew	HR OSA	Using a digital single side band comb I+jQ signal, measure the optical output image spectrum.	15
Tx IQ phs. imb. & skew	HR OSA	Using digital I+jQ with frequency notch at single side band, measure the optical spectrum at notch frequency.	16
Rx amp. resp.	Rx, ASE source	Feeding ASE noise to a coherent receiver, calculating the digital spectrum after ADC	17
Rx IQ skew	Rx, Tunable laser	Feeding CW laser to receiver and adjusting the frequency offset, estimate the phase difference between I and Q. Skew is the slope of phase difference to frequency offset.	18
In-field measurement before service.			
Tx amp. resp.	Tx, low speed PD & DSP	For an ideal MZM, the optical average power has a fixed but unknown relationship with the input electrical tone amplitude. Calibrate this relationship first and measure the Tx amplitude response by sweeping the tone frequency.	19
Tx IQ frequency dependent phs. imb.	Tx, low speed PD & DSP	Feeding $\cos(\omega t)$ to I, $\cos(\omega t + d\omega t)$ to Q, and setting IQ phase bias to zero, PD detects differential beating signal $d\omega$. The phase of the beating signal is an IQ phase imbalance.	20
Tx phs. resp.	Tx, low speed PD & DSP	Feeding $\cos(\omega t)$ and $\cos(\omega t + d\omega t)$ to one tributary, PD detects a differential beating signal $d\omega$. The phase of the beating signal is the differential phase response.	21
Tx IQ skew	Tx, low speed PD	Feeding the same BPSK signal to I and Q branches in Tx and setting IQ bias to π , the output optical average power is at its minimum if there is no IQ skew.	22
All kinds of Tx IQ imb.	Tx, high speed PD, ADC	Phase retrieval approach	23
All kinds of Tx IQ imb.	Tx, delay interferometer, high speed BPD & ADC	By feeding an elaborate IQ stimulus, the delay interferometer and balanced PD realize self-coherent detection. A frequency dependent IQ imbalance is detected.	24
Tx & Rx IQ skew	Tx, Rx	Feeding the IQ interleaved multi-tone stimulus into the transmitter, the Rx DSP simultaneously estimates the transmitter and receiver IQ skew.	25
Tx IQ skew	Tx, Rx	Using indirect learning architecture and the feedback signal after receiver carrier recovery, the transmitter IQ skew is estimated from the coefficient of transmitter adaptive pre-distortion.	26
All kinds of Rx IQ imb.	Tx, Rx	Tx generates a real value comb optical signal from a digital comb signal in either the I or Q branch. If there is a frequency offset, each tone splits into two tones after beating with the local laser at the receiver. Then, receiver IQ response and imbalance could be estimated based on receiver DSP.	27
Tx & Rx polarization skew	Tx, Rx	Employing the unitary polarization change matrix, both Tx, and Rx polarization skews are simultaneously measured by analyzing the receiver adaptive equalizer coefficient.	28
Mainly Tx imperfections	Tx, high or low speed PD&DSP	Machine learning	29-31
In-field measurement after service			
All kinds of Rx imb.	Rx	The receiver's widely linear adaptive equalizer before carrier phase recovery compensates the receiver's IQ imbalance, and the coefficient contains the information of the IQ imbalance.	10,32,33
All kinds of Tx imb.	Rx	If there is a frequency offset, Tx I and Q are mixed in the receiver. After carrier phase recovery, they are separated again. The widely linear equalizer compensates and monitors them.	10,34-36
Rx skew	Rx	Clock recovery detects the time of each tributary.	37,38

amp. = amplitude; phs. = phase; resp. = response; imb. = imbalance;

high speed means the speed of baud rate.

HR OSA: high resolution optical spectrum analyzer; BPD: balanced photo detector;

A. Overview of Device Nonlinear Imperfections, Modeling and Specifications

An optical transceiver contains many devices, and most of them could be the sources of nonlinear impairments. The gray blocks in Fig. 5(a) are the major nonlinear sources in coherent transceivers. Both DAC and ADC have integral nonlinearity. The driver and transimpedance amplifier (TIA) have nonlinear effects. The MZM has an inherent sinusoidal function which is nonlinear when the input swing is not small enough. In recent high baud rate transmissions, the multiplexed DAC or ADC is used to increase the sampling speed [1]–[3]. In such a multiplexed architecture, the imbalance between sub-DAC/ADC causes nonlinear impairment [39], [40].

Nonlinear modeling is much more complex than linear modeling. The Volterra series is the general nonlinear model [41]. It belongs to the black model because the model just describes

the input and output relationships and does not describe the actual nonlinear mechanism. The Volterra coefficients, or kernels, could be learned from the device's input and output waveform. In Volterra series, the number of terms increases with nonlinear order and memory length exponentially. To overcome this issue, various simplified models were proposed [42]. Among them, the most simplified one is the memoryless polynomial model. Besides such black box models, some models employ nonlinear physical mechanisms. For example, the MZM naturally has a sinusoidal function. Such a model is categorized as a "white model."

There are several nonlinear specifications to characterize the nonlinear effect. The definition of THD is shown in Fig. 5(b). In THD measurement, a single frequency tone is injected into the device under test, and all orders of harmonic tone are measured at output. THD is defined as $\sqrt{P_2 + P_3 + \dots} / \sqrt{P_1}$.

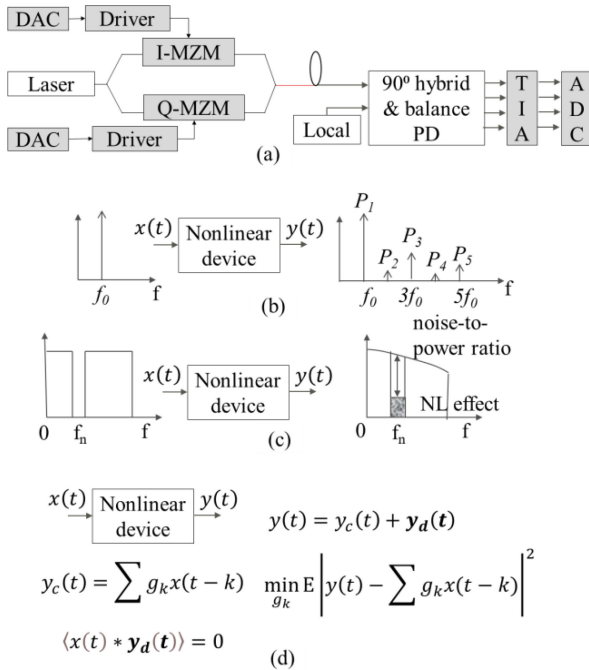


Fig. 5. Transceiver nonlinear impairment sources and device nonlinear specifications. (a) nonlinear device, (b) total harmonic distortion (c) nonlinear noise to power ratio (d) correlated component and orthogonal component.

The definition of NPR is shown in Fig. 5(c). In an NPR measurement, the component at notch frequency f_n is removed at input, and the output spectrum is measured. Since linear effects do not generate new frequency components, the output re-growth component at notch frequency can be attributed to nonlinear effects. The ratio between the re-growth component power and the signal power is NPR. This method was proposed 50 years ago [43], and is still widely used now.

The definition of correlated component and orthogonal component is shown in Fig. 5(d). The output $y(t)$ is the summation of the correlated component $y_c(t)$ and the orthogonal component $y_d(t)$. The correlated component is the best linear approximation of nonlinear output, i.e., $y_c(t) = \sum g_k x(t - k)$ where the coefficient g_k satisfies the minimum mean square error (MMSE) criterion. The orthogonal component is the left part $y_d(t) = y(t) - y_c(t)$, and the correlation between $y_d(t)$ and $x(t)$ is zero, i.e., $\langle x(t) \times y_d(t) \rangle = 0$. The correlated component is the best linear approximation of nonlinear output, whereas the orthogonal component is considered a nonlinear noise [44].

Those nonlinear specifications describe device nonlinear characteristics from different points of view. For communication systems, we care about the system performance BER or Q value. Unfortunately, nonlinear impairment does not only depend on device status but also depends on input signal characteristics, such as spectrum and PDF. The test signal for the nonlinear specification usually differs from the signal in real communication. Thus, it's hard to estimate nonlinear system performance from the nonlinear specification because the nonlinear behavior changes. In the following part, we focus on how to connect nonlinear system performance and device nonlinear characteristics.

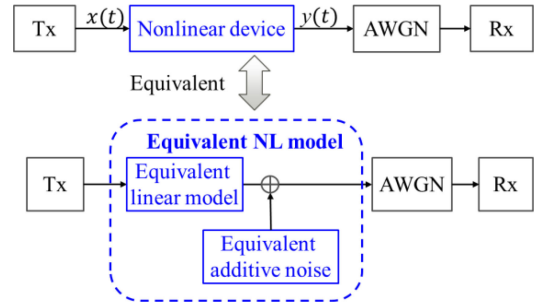


Fig. 6. Equivalent additive noise model for nonlinear system, AWGN: additive white Gaussian noise.

B. Equivalent Additive Noise Model

Basically, nonlinear distortion is a deterministic distortion. Different input signal bit patterns have different nonlinear distortions. This causes many difficulties in nonlinear system performance estimation. To solve this issue, we proposed an equivalent additive noise model in [45]. Fig. 6 shows the concepts where the nonlinear device is approximated as an equivalent linear model and an equivalent additive noise. The nonlinear distortion is described by the equivalent additive noise, and such noise is independent on the input signal bit pattern. It is not difficult to estimate the system performance from the equivalent additive noise model because it is a linear system. The problem turns to how to obtain the equivalent linear model and equivalent additive noise so that the estimated system performance is close to the actual nonlinear system performance. In order to focus on nonlinear effects, we assume the receiver has an ideal linear equalizer.

C. Total Harmonic Distortion and Nonlinear Terms

In THD, the harmonic terms are considered a nonlinear distortion. Thus, it is straightforward to consider a nonlinear term as the equivalent additive noise. The first drawback of THD is the low input frequency. Since THD needs the measurement of all harmonics, the input signal frequency is usually limited by the scope of the spectrum analyzer. This is not a big issue if the device nonlinearity is frequency independent. However, the device in an optical coherent transceiver has a very wide bandwidth, and the nonlinear effect strongly depends on the input signal frequency. For example, a 40 dB frequency dependency of nonlinear effects was observed in the TIA of a coherent receiver [46]. Thus, THD is not a suitable specification for nonlinear devices in optical communications.

Counter-intuitively, nonlinear terms cannot be considered a nonlinear noise, i.e., the equivalent additive noise in the model, in general [45]. The experimental verification of the equivalent additive noise model is shown in Fig. 7. The device under test is an electrical driver designed for an optical coherent transmitter. The transmitted signal is 42 GBaud PAM8 with a Nyquist roll off factor of 0.15. We established the Volterra models, which have 301 taps of linear terms, 15 taps of 2nd order nonlinear terms, and 9 taps of 3rd order nonlinear terms for that device. The waveform estimated by the Volterra model and the actual

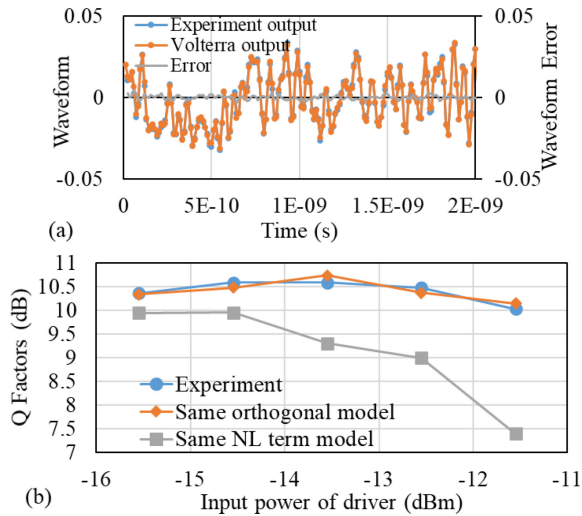


Fig. 7. Performance of the equivalent additive noise model for the electrical driver in an optical transmitter: (a) Volterra model accuracy for the driver (b) system performance estimation using the same orthogonal model and the same nonlinear term model.

waveform is shown in Fig. 7(a). The Volterra model error is as low as -29 dB. The gray square in Fig. 7(b) shows the performance of the same nonlinear term model where the linear term in the Volterra series is considered an equivalent linear model and the nonlinear term is considered an equivalent additive noise. In order to guarantee the independence of the noise from the input signal bit pattern, the nonlinear term of one bit pattern is used as the equivalent noise of another input signal bit pattern. Nonlinear terms cannot be considered a nonlinear noise, as shown in Fig. 7(b). The reason is that nonlinear terms also contain the information of an input signal. Taking the simplest 3rd order polynomial model $y = x + cx^3$ as an example, the correlation between the nonlinear term cx^3 and the input signal x is $\langle cx^3x \rangle = \langle c|x|^4 \rangle$ which is not zero. The preceding analysis shows that even orders of nonlinear terms can be considered an equivalent additive noise, which is supported by simulation [45].

D. Orthogonal Components

Orthogonal component analysis is widely used in wireless communication and is explained in [44]. The basic idea is to decompose the nonlinear device's output signal into correlated and orthogonal components. The correlated component could be generated by a linear process of the input signal, and the orthogonal component cannot be generated by any linear process. If we have the nonlinear device input signal $x(t)$ and output signal $y(t)$, the correlated component and the orthogonal component can be obtained by the MMSE estimation method, as shown in Fig. 5. Many earlier works can be found in [47]–[49].

Accurate measurement of the orthogonal component is difficult. It needs precise comparison of nonlinear device input and output signals, which requires expensive instruments such as AWG and DSO. In the time domain, if the digital samples of the input and output signals are measured, the orthogonal component could be calculated by its definition [45], [50].

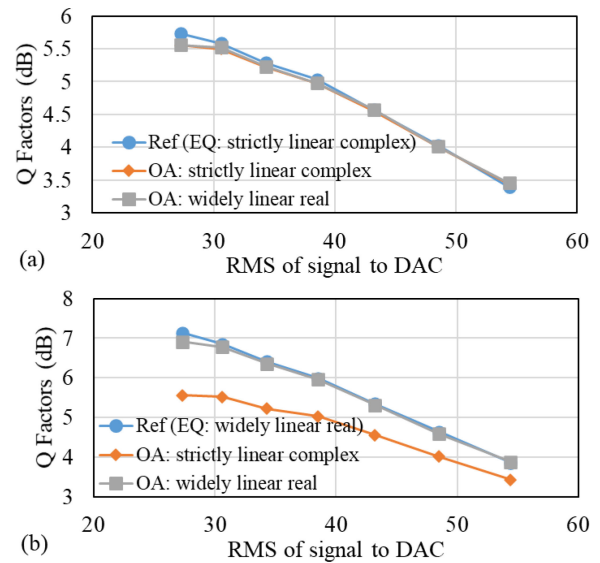


Fig. 8. Selection of the receiver equalizer affects the selection of orthogonal analysis. (a) Strictly linear complex equalizer in receiver (b) widely linear real equalizer in receiver. Ref: reference performance by actual nonlinear system, EQ: equalizer; OA: estimated performance by different orthogonal analysis process.

Alternatively, the orthogonal component analysis could be performed in the frequency domain [51]. In addition, the orthogonal component is the small difference between two large signals. A small measurement error in the input or output signals causes a large measurement error in the orthogonal component.

Since orthogonal components cannot be generated by any linear process, it's reasonable to consider orthogonal components as the equivalent additive noise, and we name this method the same orthogonal model. The equivalent linear model could be obtained by the correlated component, i.e., the coefficients g_k . In order to guarantee the independence of equivalent additive noise, the orthogonal component of one bit pattern is used as the equivalent noise of another input bit pattern. A more simplified solution is the time-circle-shift of orthogonal components. The nonlinear system performance estimated by the same orthogonal model is shown in Fig. 7(b). The estimation accuracy reaches 0.2 dB, which is quite good.

In the case of optical coherent communication, the orthogonal component analysis becomes more complex. Orthogonal analysis should consider the receiver linear equalizer selection. In the optical coherent receiver, there are two kinds of linear equalizer. The first one is a strictly linear complex signal equalizer. It compensates for chromatic dispersion and polarization mode dispersion, but it cannot compensate for an IQ imbalance. The other one is a widely linear real signal equalizer, which compensates for imperfections in the I, Q, and IQ branches. The widely linear equalizer has better performance than the strictly linear equalizer, but the complexity and power consumption are higher. The equivalent linear model in orthogonal analysis (OA) also has two options: a strictly linear complex model and a widely linear real model.

The experimental result of the same orthogonal model for optical coherent back-to-back transmission is shown in Fig. 8.

The system parameters are dual-polarization 44 GBaud 64QAM with a Nyquist roll off factor of 0.15. In the experiment, the amplitude of the transmitter digital signal was adjusted to emulate different nonlinear impairments. High amplitude means a large nonlinear impairment and a small Q factor thereafter. This amplitude is described by the root mean square (RMS) value of the digital signal to the DAC, whose full swing is -127 to 127 . The case of strictly linear complex equalizer in the receiver is shown in Fig. 8(a), while that of the widely linear real equalizer is shown in (b). Interestingly, the estimated performance by both strictly linear complex OA and widely linear real OA agrees with the actual nonlinear system performance if the receiver uses a strictly linear complex equalizer. However, if the receiver uses a widely linear real equalizer, only the widely linear real OA agrees, and there is a large error in the strictly linear complex OA.

The reason for such an interesting phenomenon is the IQ imbalance. In reality, an IQ imbalance always exists. In the strictly linear complex OA, the IQ imbalance is included in the orthogonal component and the equivalent additive noise thereafter. In the widely linear real OA, the IQ imbalance is included in the linear model, but not in the equivalent additive noise.

If the receiver equalizer is strictly linear, it cannot compensate for the IQ imbalance in reality. It also cannot compensate for the IQ imbalance in nonlinear system performance estimation, whether the IQ imbalance is included in the equivalent linear model (widely linear real OA) or the equivalent additive noise (strictly linear complex OA). Thus, Fig. 8(a) shows the three curves agree with each other.

However, if the receiver equalizer is widely linear, it compensates for the IQ imbalance in reality. In the nonlinear system performance estimation, the equalizer compensates for the IQ imbalance that is included in the linear model (widely linear real OA) but cannot compensate for the IQ imbalance that is included in the equivalent additive noise (strictly linear complex OA). Thus, the curve of widely linear real OA agrees with the actual performance, but the curve of strictly linear complex OA underestimates the system performance.

In short, nonlinear system performance estimated by the same orthogonal model agrees with the actual performance. The drawback of this method is the difficulties in orthogonal component measurement. In addition, the type of receiver equalizer affects the selection of OA in optical coherent communication. It's safe to select the same process in receiver equalizer and orthogonal component analysis.

E. Nonlinear Noise to Power Ratio

The linear effect does not generate any new frequency components, so that NPR is a straightforward nonlinear specification. Compared with the orthogonal component, NPR could be measured easily by a spectrum analyzer. With DSP technology, the deep notch of the input signal is not difficult. In addition, NPR could be used for a device with different input and output signal types. For example, an optical coherent driver modulator has an electrical input signal and an optical output signal. It's very hard to do OA on such a device.

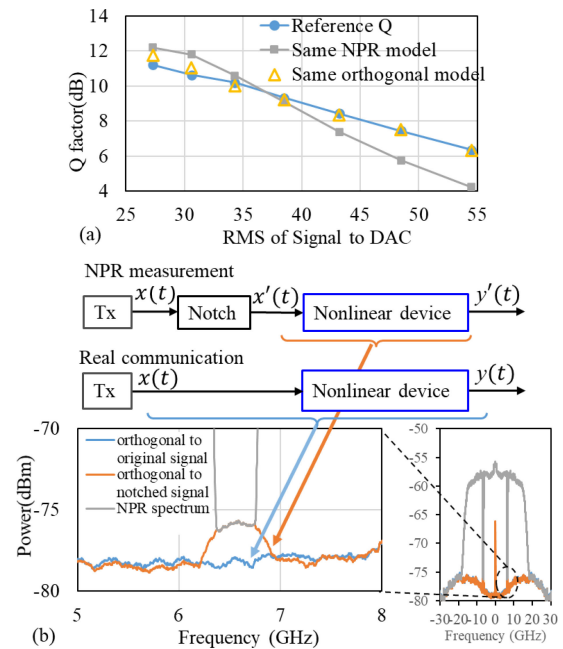


Fig. 9. The same NPR model does not provide the correct nonlinear system performance estimation. (a) System performance. (b) The failure is caused by the notch process, which alters the orthogonal component.

Unfortunately, the same NPR model that sets the spectrum of equivalent additive noise as the NPR measurement result cannot correctly estimate the actual nonlinear system performance in general [52]. The experimental result is shown in Fig. 9. The nonlinear device is an electrical driver for an optical coherent transmitter whose dominant nonlinear distortion is 3rd order nonlinearity. The system is 31.5 GBaud PAM8 with a Nyquist roll off factor of 0.15. The same orthogonal model agrees with the actual reference Q value while the same NPR model does not agree as shown in Fig. 9(a).

The reason for the disagreement is shown in Fig. 9(b). In real communication, the input signal is $x(t)$ and the output is $y(t)$. We calculate the orthogonal component in this case, and the spectrum of the orthogonal component is shown by the blue curve (orthogonal to the original signal). This is the correct orthogonal component. In NPR measurement, we notch the original signal $x(t)$ and the nonlinear device input signal is the notched signal $x'(t)$. Then, the output signal is $y'(t)$. The NPR method measures the spectrum of $y'(t)$ and the spectrum is shown by the gray curve (NPR spectrum). We also calculate the orthogonal component of the notched signal $x'(t)$ and the nonlinear output $y'(t)$. The orange curve (orthogonal to the notched signal) shows the spectrum. The gray curve agrees with the orange curve at the notch frequency, which implies that NPR correctly measures the orthogonal component of the notched signal $x'(t)$. However, there is a gap between the orange curve and the blue curve. In other words, the notch process itself changes the orthogonal component. Interestingly, such a change only occurs at notch frequency, but NPR only measures the spectrum at notch frequency. Thus, NPR cannot correctly measure the orthogonal component of actual communication, and this causes the system performance estimation error.

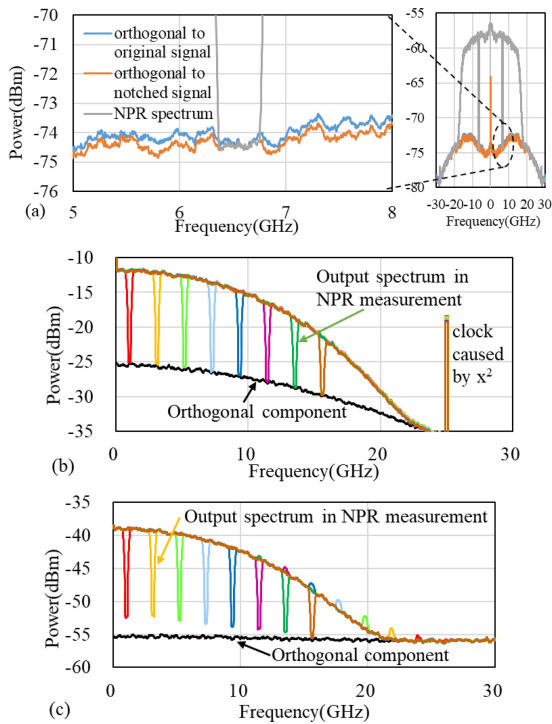


Fig. 10. The cases (a and b) where NPR provides the correct orthogonal components (a) nonlinear system with Gaussian input, (b) 2nd order polynomial with PAM4 input, and (c) 3rd order polynomial with PAM4 input.

There are some special but still useful cases where NPR provides the correct orthogonal component and the same NPR model estimates nonlinear system performance correctly. The result of Gaussian input is shown in Fig. 10(a). The nonlinear device is the same as that in Fig. 9, but the input signal changes from PAM8 to a random Gaussian symbol. In this case, the three curves, i.e., the orthogonal component of the original signal, the orthogonal component of the notched signal, and the spectrum of NPR, agree well with each other. In fact, Gaussian input is the request of the NPR application. The mathematical explanation can be found in [53]. Fig. 10(b) shows the result of a 2nd order polynomial system $y(t) = C_1 x(t) + C_2 x^2(t)$. The input signal is 25 GBaud PAM4 with a Nyquist roll off of 1. Since the signal and system are real, only the positive spectra are shown. It's clear that the NPR measures the orthogonal component correctly even when the input signal is non-Gaussian. The spike at 25 GHz is caused by the 2nd order nonlinear term. In fact, square operations can be used for clock recovery [54]. In practical optical communication, the nonlinear distortion in IM/DD systems is usually dominated by the 2nd order term. In such a case, the NPR method works correctly [55]. For comparison, Fig. 10(c) shows the result of a 3rd order polynomial system $y(t) = C_1 x(t) + C_2 x^2(t) + C_3 x^3(t)$. The NPR result does not match the orthogonal component. The coefficient values of C_1 , C_2 , and C_3 are 0.476, $-1.63e-3$, and $-2.45e-3$, respectively. In optical coherent communication systems, the dominant nonlinear distortion is a 3rd order term, and the NPR method does not work.

F. Summary of Device Nonlinear Imperfections

Device nonlinear imperfections are an important but complicated impairment in optical coherent transceivers. There are various nonlinear specifications such as THD, nonlinear term, orthogonal component, and NPR. For communication systems, it's desired that the nonlinear system performance could be estimated practically from nonlinear specifications. Using the equivalent additive noise model, the same orthogonal model accurately estimates nonlinear system performance. However, the measurement of the orthogonal component is quite challenging. NPR can be easily measured, but the same NPR model cannot always correctly estimate nonlinear system performance. In some special but still useful cases, for example, Gaussian input, even order nonlinear system, the same NPR model is correct.

IV. CONCLUSION

Device imperfections in transceivers are found to be the primary source of impairment in high baud rate, high order format optical communication systems. Linear imperfections are relatively easy to characterize, model, and measure. Linear imperfections could be precisely measured in a laboratory by instruments. In-field measurement is necessary because the device's imperfection may change with the environment. Many methods for measuring linear flaws without instruments have been proposed, using additional devices and DSP. Among these, the methods with low speed devices and DSP are preferred. In the case of nonlinear imperfections, the situation is complex. There have been various nonlinear specifications and corresponding measurements. For communication systems, it is desirable to practically estimate nonlinear system performance based on the nonlinear characteristics of the devices. The orthogonal component has a good correlation with nonlinear system performance, although it is difficult to measure. The NPR is easy to measure, but it does not correctly estimate the nonlinear system performance in general. The NPR is correct in some special but useful cases, such as Gaussian input signals and even order nonlinear systems.

REFERENCES

- [1] Q. Hu *et al.*, "Plasmonic-MZM-based short-reach transmission up to 10 km supporting >304 GBd polybinary or 432 Gbit/s PAM-8 signaling," in *Proc. 47th Eur. Conf. Opt. Commun. (ECOC) Postdeadline Pap.*, Bordeaux, France, 2021, Paper Th3C1-PD2.4.
- [2] F. Pittalà *et al.*, "220 GBaud signal generation enabled by a two-channel 256 GSa/s arbitrary waveform generator and advanced DSP," in *Proc. Eur. Conf. Opt. Commun.*, Brussels, Belgium, 2020, Paper Th3A.4.
- [3] M. Nakamura *et al.*, "192-GBaud signal generation using ultra-broadband optical frontend module integrated with bandwidth multiplexing function," in *Proc. Opt. Fiber Commun. Conf. (OFC) Postdeadline Papers*, San Diego, CA, USA, 2019, Paper Th4B.4.
- [4] Y. Wakayama *et al.*, "2048-QAM transmission at 15 GBd over 100 km using geometric constellation shaping," *Opt. Exp.*, vol. 29, no. 12, pp. 18743–18759, 2021.
- [5] F. Pittalà *et al.*, "1.71 Tb/s single-channel and 56.51 Tb/s DWDM transmission over 96.5 km field-deployed SSMF," 2021, arXiv:2108.01873.
- [6] M. Nakamura *et al.*, "1.3-Tbps/carrier net-rate signal transmission with 168-GBaud PDM PS-64QAM using analogue-multiplexer-integrated optical frontend module," in *Proc. 45th Eur. Conf. Opt. Commun. (ECOC)*, Dublin, Ireland, 2019, Paper Tu2D.5.

- [7] K. Schuh *et al.*, "Single carrier 1.2 Tbit/s transmission over 300 km with PM-64 QAM at 100 GBaud," in *Proc. Opt. Fiber Commun. Conf.*, Los Angeles, CA, USA, 2017, Paper Th5B.5.
- [8] Z. Tao *et al.*, "Characterization, modelling and measurement of device imperfections in advanced coherent transceivers," in *Proc. 47th Eur. Conf. Opt. Commun.*, Bordeaux, France, 2021, Paper Tu3C2.1.
- [9] M. G. Khaled, "Nonlinear system figures of merit," in *Nonlinear Distortion in Wireless Systems: Modeling and Simulation With Matlab*, Chichester, West Sussex, U.K.: Wiley, 2012, pp. 158–173.
- [10] M. Paskov, D. Lavery, and S. J. Savory, "Blind equalization of receiver in-phase/quadrature skew in the presence of Nyquist filtering," *IEEE Photon. Technol. Lett.*, vol. 25, no. 24, pp. 2446–2449, Dec. 2013.
- [11] E. P. Da Silva and D. Zibar, "Widely linear equalization for IQ imbalance and skew compensation in optical coherent receivers," *J. Lightw. Technol.*, vol. 34, no. 15, pp. 3577–3586, 2016.
- [12] C. R. S. Fludger and T. Kupfer, "Transmitter impairment mitigation and monitoring for high baud-rate, high order modulation systems," in *Proc. 42nd Eur. Conf. Opt. Commun.*, Dusseldorf, Germany, 2016, Paper Tu2A.2.
- [13] L. Anttila, M. Valkama, and M. Renfors, "Frequency-selective I/Q mismatch calibration of wideband direct-conversion transmitters," *IEEE Trans. Circuits Syst., II, Exp. Briefs*, vol. 55, no. 4, pp. 359–363, Apr. 2008.
- [14] J. Qi, B. Mao, N. Gonzalez, L. N. Binh, and N. Stojanovic, "Generation of 28GBaud and 32GBaud PDM-Nyquist-QPSK by a DAC with 11.3 GHz analog bandwidth," in *Proc. Opt. Fiber Commun. Conf. Nature Fiber Opt. Engi. Conf.*, Anaheim, CA, USA, 2013, Paper OTh1F.1.
- [15] H. Chen *et al.*, "An accurate and robust in-phase/quadrature skew measurement for coherent optical transmitter by image spectrum analyzing," in *Proc. 43rd Eur. Conf. Opt. Commun.*, Gothenburg, Sweden, 2017, Paper P1.SC3.35.
- [16] F. J. Vaquero-Caballero, D. J. Ives, and S. J. Savory, "Transceiver noise characterization based on perturbations," *J. Lightw. Technol.*, vol. 39, no. 18, pp. 5799–5804, 2021.
- [17] A. Matsushita, M. Nakamura, F. Hamaoka, S. Okamoto, and Y. Kisaka, "High-spectral-efficiency 600-Gbps/carrier transmission using PDM-256QAM format," *J. Lightw. Technol.*, vol. 37, no. 2, pp. 470–476, 2019.
- [18] Implementation agreement for analogue coherent optics module, OIF-CFP2-ACO-01.0, optical internetworking forum (OIF), 2016. [Online]. Available: <https://www.oiforum.com/technical-work/implementation-agreements-ias/>
- [19] Y. Fan *et al.*, "Overall frequency response measurement of DSP-Based optical transmitter using built-in monitor photodiode," in *Proc. 42nd Eur. Conf. Opt. Commun.*, Dusseldorf, Germany, 2016, Paper Th2.P2.SC4.5.
- [20] C. R. S. Fludger, T. Duthel, P. Hermann, and T. Kupfer, "Low cost transmitter self-calibration of time delay and frequency response for high baud-rate QAM transceivers," in *Proc. Opt. Fiber Commun. Conf.*, Los Angeles, CA, USA, 2017, Paper Th1D.3.
- [21] Y. Fan, Z. Tao, H. Nakashima, and T. Hoshida, "In-field calibration of phase response of optical transmitter using built-in monitor photodiode," in *Proc. Opt. Fiber Commun. Conf.*, San Francisco, CA, USA, 2021, Paper Th5D.4.
- [22] Y. Yue *et al.*, "Detection and alignment of dual-polarization optical quadrature amplitude transmitter IQ and XY skews using reconfigurable interference," *Opt. Exp.*, vol. 24, no. 6, pp. 6719–6734, 2016.
- [23] Y. Yoshida, S. Yoshida, S. Oda, T. Hoshida, and N. Yamamoto, "Simultaneous monitoring of frequency-dependent IQ imbalances in a dual-polarization IQ modulator by using a single photodetector: A phase retrieval approach," in *Proc. Opt. Fiber Commun. Conf.*, San Francisco, CA, USA, 2021, Paper Th5D.2.
- [24] X. Chen and D. Che, "Direct-detection based frequency-resolved I/Q imbalance calibration for coherent optical transmitters," in *Proc. Opt. Fiber Commun. Conf.*, San Francisco, CA, USA, 2021, Paper Th5D.3.
- [25] D. Li *et al.*, "Simultaneously precise calibration of frequency response and IQ skew for 100 Gbaud optical transceiver," in *Proc. Opt. Fiber Commun. Conf.*, San Francisco, CA, USA, 2021, Paper Th5D.1.
- [26] G. Khanna, B. Spinnler, S. Calabrò, E. De Man, and N. Hanik, "A robust adaptive pre-distortion method for optical communication transmitters," *IEEE Photon. Technol. Lett.*, vol. 28, no. 7, pp. 752–755, Apr. 2016.
- [27] C. Ju *et al.*, "Calibration of in-phase/quadrature amplitude and phase response imbalance for coherent receiver," in *Proc. Opt. Fiber Commun. Conf.*, Los Angeles, CA, USA, 2017, Paper W2A.55.
- [28] Y. Jiang *et al.*, "Calibration of polarization skews in optical coherent transceiver based on digital signal processing," in *Proc. 45th Eur. Conf. Opt. Commun.*, Dublin, Ireland, 2019, Paper Th1B2.
- [29] X. Dai, X. Li, M. Luo, and S. Yu, "Numerical simulation and experimental demonstration of accurate machine learning aided IQ time-skew and power-imbalance identification for coherent transmitters," *Opt. Exp.*, vol. 27, no. 26, pp. 38367–38381, 2019.
- [30] S. Savian *et al.*, "Joint estimation of IQ phase and gain imbalances using convolutional neural networks on eye diagrams," in *Proc. Conf. Lasers Electro-Opt.*, San Jose, CA, USA, 2018, Paper STh1C.3.
- [31] Q. Zhang *et al.*, "Algorithms for blind separation and estimation of transmitter and receiver IQ imbalances," *J. Lightw. Technol.*, vol. 37, no. 10, pp. 2201–2208, 2019.
- [32] M. S. Faruk and S. J. Savory, "Digital signal processing for coherent transceivers employing multilevel formats," *J. Lightw. Technol.*, vol. 35, no. 5, pp. 1125–1141, 2017.
- [33] R. Rios-Müller, J. Renaudier, and G. Charlet, "Blind receiver skew compensation and estimation for long-haul non-dispersion managed systems using adaptive equalizer," *J. Lightw. Technol.*, vol. 33, no. 7, pp. 1315–1318, 2015.
- [34] Y. Fan *et al.*, "Experimental verification of IQ imbalance monitor for high-order modulated transceivers," in *Proc. 44th Eur. Conf. Opt. Commun.*, Rome, Italy, 2018, Paper Th1D.5.
- [35] Y. Fan *et al.*, "Transceiver IQ imperfection monitor by digital signal processing in coherent receiver," in *Proc. 24th Optoelectron. Commun. Conf. Int. Conf. Photon. Switch. Comput.*, Fukuoka, Japan, 2019, Paper ThC2-1.
- [36] J. Liang, Y. Fan, Z. Tao, X. Su, and H. Nakashima, "Transceiver imbalances compensation and monitoring by receiver DSP," *J. Lightw. Technol.*, vol. 39, no. 17, pp. 5397–5404, 2021.
- [37] N. Stojanovic and X. Changsong, "An efficient method for skew estimation and compensation in coherent receivers," *IEEE Photon. Technol. Lett.*, vol. 28, no. 4, pp. 489–492, Feb. 2016.
- [38] P. Skvortcov, C. Sanchez-Costa, I. Phillips, and W. Forsyiaik, "Joint Tx and Rx skew calibration in coherent transceivers based on Rx-side DSP," in *Proc. IEEE Photon. Conf.*, Reston, VA, USA, 2018, Paper TuA1.3.
- [39] E. Olieman, A. Annema, and B. Nauta, "An interleaved full Nyquist high-speed DAC technique," *IEEE J. Solid State Circuits*, vol. 50, no. 3, pp. 704–713, Mar. 2015.
- [40] C. Han, K. Igarashi, and K. Kikuchi, "Influence of channel misalignment of time-interleaved DAC on sensitivity degradation in coherent optical receivers," in *Proc. Opt. Fiber Commun. Conf. Expo. Nature Fiber Opt. Engineers Conf.*, Anaheim, CA, USA, 2013, Paper OTh1F.2.
- [41] S. Narayanan, "Transistor distortion analysis using volterra series representation," *Bell Syst. Tech. J.*, vol. 46, no. 5, pp. 991–1024, 1967.
- [42] F. M. Ghannouchi and O. Hammi, "Behavioral modeling and predistortion," *IEEE Microw. Mag.*, vol. 10, no. 7, pp. 52–64, Dec. 2015.
- [43] R. W. Koch, "Random signal method of nonlinear amplitude distortion measurement," *IEEE Trans. Instrum. Meas.*, vol. IM-20, no. 2, pp. 95–99, May 1971.
- [44] M. G. Khaled, "Nonlinear distortion," in *Nonlinear Distortion in Wireless Systems: Modeling and Simulation With Matlab*, Chichester, West Sussex, U.K.: Wiley, 2012, pp. 131–157.
- [45] X. Su *et al.*, "Accurate performance estimation for nonlinear system," in *Proc. 26th Optoelectron. Commun. Conf.*, 2021, Paper W2A.3.
- [46] Z. Tao *et al.*, "Nonlinear characteristic of wideband coherent receiver and the application of Wiener-Hammerstein model," in *Proc. Asia Commun. Photon. Conf.*, Chengdu, China, 2019, Paper S4B.4.
- [47] J. Schoukens, R. Pintelon, T. Dobrowiecki, and Y. Rolain, "Identification of linear systems with nonlinear distortions," *Automatica*, vol. 41, no. 3, pp. 491–504, 2005.
- [48] S. Klein and S. Yasui, "Nonlinear systems analysis with non-Gaussian white stimuli; general basis functionals and kernels (Corresp.)," *IEEE Trans. Inf. Theory*, vol. 25, no. 4, pp. 495–500, Jul. 1979.
- [49] R. J. Fenton, "Noise-loading analysis for a general memoryless system," *IEEE Trans. Instrum. Meas.*, vol. 26, no. 1, pp. 61–64, Mar. 1977.
- [50] F. Ramian, "Amplifier characterization using non-CW stimulus," in *Proc. IEEE Int. Workshop Metrol. Aerosp. (MetroAeroSpace)*, Padua, Italy, 2017, pp. 198–200.
- [51] J. Verspecht, A. Stav, J. Teysier, and S. Kusano, "Characterizing amplifier modulation distortion using a vector network analyzer," in *Proc. 93rd AFTG Microw. Meas. Conf.*, Boston, MA, USA, 2019, pp. 1–4.
- [52] Z. Tao, K. Zhang, X. Su, H. Nakashima, and T. Hoshida, "Nonlinear noise measurement for optical communication," in *Proc. 26th Optoelectron. Commun. Conf. (OECC)*, 2021, Paper W2A.5.
- [53] K. M. Gharaibeh, "On the relationship between the Noise-to-Power ratio (NPR) and the effective in-Band distortion of WCDMA signals," *AEU Int. J. Electron. Commun.*, vol. 64, no. 3, pp. 273–279, 2010.
- [54] L. F. and J. B., "Statistical properties of timing jitter in a PAM timing recovery scheme," *IEEE Trans. Commun.*, vol. 22, no. 7, pp. 913–920, Jul. 1974.
- [55] C. Yang *et al.*, "A simple and accurate method to estimate the nonlinear performance of VCSEL IM-DD system," in *Proc. Opt. Fiber Commun. Conf.*, 2022, Paper W2A.34.